1996SoPh..164..253S

THE INFLUENCE OF SUNSPOT CANOPIES ON MAGNETIC INCLINATION MEASUREMENTS IN SOLAR PLAGES

SAMI K. SOLANKI, WOLFGANG FINSTERLE and ISABELLE RÜEDI
Institute of Astronomy, ETH Zentrum, CH-8092 Zurich, Switzerland

Abstract. Sunspots are known to have large, low-lying magnetic canopies, i.e. horizontal magnetic fields overlying a field-free medium, that cover substantial fractions of active region plage. In this paper we consider the influence of such canopies on the inclination of plage magnetic fields. We find that for observations in spectral lines like 5250.2Å the neglect of a sunspot canopy when determining magnetic inclination angles of plage fields can introduce errors exceeding 5–10°. This is particularly true if the observations do not have high spatial resolution. Thus this effect may explain some of the measurements of substantially inclined fields in solar plages. Furthermore we find that the Fe I 15648 Å line is far superior in giving correct flux-tube inclinations in the presence of a sunspot magnetic canopy. Finally, the inversion of full Stokes profiles is shown to produce more reliable results than results obtained by considering only ratios of individual Stokes profile parameters.

Key words: Magnetic fields – active regions – plage – sunspots – flux tubes

1. Introduction

Reliable observations of solar vector magnetic fields are central to the understanding of solar MHD processes, as testified by the increasing efforts being undertaken to derive magnetic vectors with high precision from measured Stokes profiles.

One of the important parameters one wishes to determine is the inclination angle γ' (relative to the surface normal) of the magnetic elements composing solar plages.* Initial theoretical estimates (e.g. Schüssler, 1986) predicted that kG magnetic elements should not deviate from the vertical direction by more than 1°. Later, Schüssler (1990) allowed for the possibility that some magnetic elements, those with lower field strengths, may be more strongly inclined. More recently these estimates have had to be revised in the light of the discovery of supersonic flows in solar granulation (e.g. Cattaneo *et al.*, 1990, Nesis *et al.*, 1992, Solanki *et al.*, 1995a). The increased strength of the granular buffeting can tilt individual flux tubes by as much as 15–25° (Solanki, 1993). Finally, 2-D MHD simulations (Steiner *et al.*, 1995) have demonstrated directly that flux tubes become periodically

* Primed quantities, inclination angle γ' and azimuth χ', refer to local solar coordinates, unprimed ones to inclinations and azimuths relative to the line of sight.

Solar Physics **164**: 253–264, 1996.
© 1996 *Kluwer Academic Publishers. Printed in Belgium.*

© Kluwer Academic Publishers • Provided by the NASA Astrophysics Data System

1996SoPh..164..253S

inclined by large amounts due to granular buffeting. This mechanism is expected to act on each flux tube individually, so that at any given moment the average inclination of a sufficiently large ensemble of flux tubes is expected to be small. In addition, further simulations by Steiner, Grossmann-Doerth, Knölker and Schüssler (private communication) show that only small flux tubes (diameter $\lesssim$ 400 km in the continuum forming layer) react strongly to granular buffeting. Larger flux tubes remain basically vertical throughout their simulation.

In the quiet magnetic network only an upper limit of 10° on the *average* inclination of magnetic elements is known from direct measurement (Sánchez Almeida & Martínez Pillet, 1994), although Murray (1992) finds evidence for on average highly inclined weak magnetic field from a statistical analysis of full-disk magnetograms, in particular of the centre-to-limb variation of the magnetogram signal. How far his results near the limb are affected by horizontal canopy fields due to the quiet network (Jones & Giovanelli, 1983) is an open question.

In active region plages recent observations, even when averaged over many magnetic elements, give inclinations to the vertical that often are larger than 10° (Solanki *et al.*, 1987; Lites & Skumanich, 1990; Bernasconi *et al.*, 1995). A statistical study of magnetograms (Howard, 1991) also indicates large inclinations, with the opposite polarity fields in active regions being inclined by 16° towards each other.

Although theory and quiet-sun observations are mutually consistent, they disagree with active region observations. In the present paper we investigate a possible explanation for this discrepancy. In addition to small-scale magnetic features active regions contain sunspots which possess large-scale, low-lying magnetic canopies that cover a significant fraction of active region plages (e.g. Giovanelli, 1980; Giovanelli & Jones, 1982; Solanki *et al.*, 1992b, 1994; Bruls *et al.*, 1995). We investigate how such a low-lying magnetic canopy influences and possibly falsifies magnetic element inclinations derived from the Stokes vector.

2. Technique

We have carried out a large set of calculations of Stokes parameters in a simple 2-component model of a horizontal superpenumbral magnetic canopy (1st component) and vertical magnetic elements, modelled as flux tubes (2nd component). Each magnetic component is described by a simple 1-D (i.e. plane-parallel) atmosphere. For the canopy this is clearly a reasonable assumption, while for the flux tubes its validity, as far as the inclination of the magnetic field is concerned, has been shown to hold using 2-D models (Solanki *et al.*, 1995b).

© Kluwer Academic Publishers • Provided by the NASA Astrophysics Data System

1996SoPh..164..253S

The magnetic field of the canopy, with strength B_c and an inclination to the surface normal $\gamma'_c = 90°$, is homogeneous above the canopy base-height Z_c and disappears below Z_c. The magnetic field of the flux tube has $\gamma'_{FT} = 0°$ and a strength B_{FT} whose vertical variation is given by the thin-tube approximation (Defouw, 1976). Thus in this model there is a magnetic field everywhere above the height Z_c, while below this height only the fraction of the solar surface covered by flux tubes, α_{FT}, has a magnetic field. Consequently the filling factor of the canopy component $\alpha_c = 1 - \alpha_{FT}$. In accordance with previous work the thermal structure of the canopy component is the same as that of the quiet sun (Maltby *et al.*, 1986), while the flux-tube atmosphere is described by the plage flux-tube model of Solanki & Brigljević (1992). In the present simple model pressure balance is not enforced across the canopy boundary.

At a given heliocentric angle θ we calculate the Stokes profiles for each component separately (obtaining S_{FT} and S_c, where $S = I, Q, U, V$), weight them by the surface filling factor of the respective component and add them together, forming

$$S_{tot} = S_{FT}\ \alpha_{FT} + S_c(1 - \alpha_{FT})\ .$$

In order to determine the inclination γ with respect to the line-of-sight we take two approaches. In the first the ratio $R = V/\sqrt{Q^2 + U^2}$ is used as a measure of γ. The difference between

$$R_{tot} = \frac{V_{tot}}{\sqrt{Q^2_{tot} + U^2_{tot}}}$$

and

$$R_{FT} = \frac{V_{FT}}{\sqrt{Q^2_{FT} + U^2_{FT}}}$$

is an indication of the error, $\Delta\gamma_{FT}$, introduced into γ measurements of the flux-tube field by neglecting the magnetic canopy. To estimate $\Delta\gamma_{FT}$ we have calculated R_{FT} for a number of γ'_{FT} values for each θ (i.e. flux tubes with different inclinations to the vertical; primed quantities refer to the local solar coordinate system). If γ_1 is the inclination with respect to the line of sight of the original flux tube (whose Stokes spectrum is added to that of the canopy) and γ_2 is the inclination of the flux tube that gives the same R value as R_{tot}, then $\Delta\gamma_{FT} = \mid \gamma_2 - \gamma_1 \mid$.

In the second approach we have used the inversion code described by Solanki *et al.* (1992b, 1994) to fit the combined Stokes profiles S_{tot} with a pure flux-tube model. The code then gives us γ_{FT} (fit) and χ_{FT} (fit), which can be compared with the true values to yield $\Delta\gamma_{FT}$ and $\Delta\chi_{FT}$. Here χ is

© Kluwer Academic Publishers • Provided by the NASA Astrophysics Data System

1996SoPh..164..253S

the magnetic azimuth. We define $\chi = \chi' = 0$ in the direction of solar disk centre.

We have calculated the Stokes profiles of four Fe I spectral lines using the Stokes transfer code of Solanki *et al.* (1992a) based on the Diagonal Element Lambda Operator (DELO) technique (Rees *et al.*, 1989; Murphy, 1990). The four lines are: 5247.1Å (excitation potential $\chi_e = 0.09$ eV, Landé factor $g_{\rm eff} = 2$), 5250.2Å ($\chi_e = 0.12$ eV, $g = 3$), 5250.6Å ($\chi_e = 2.20$ eV, $g_{\rm eff} = 1.5$) and 15648Å ($\chi_e = 5.43$ eV, $g = 3$). The three lines in the visible have been shown to be very useful diagnostics of the field strength and the temperature in small-scale magnetic features by Stenflo *et al.* (1987) and Zayer *et al.* (1990).

The free parameters of the model calculations are: Z_c, $\alpha_{\rm FT}$, B_c, $B_{\rm FT}$, $\xi_{\rm mac}$, χ'_c, where $\xi_{\rm mac}$ is the macroturbulence velocity and χ'_c is the azimuthal angle of the canopy magnetic field in local (solar) coordinates. We have carried out model calculations for $Z_c = 300$, 400 and 500 km, with the corresponding B_c values 500, 300 and 200 G. This Z_c–B_c combination corresponds roughly to values derived from infrared lines (Solanki *et al.*, 1992b, 1994; Hewagama *et al.*, 1993 and Bruls *et al.*, 1994). Following the constraints imposed by observations (e.g. Rüedi *et al.*, 1992), only a single value of $B_{\rm FT}$, namely $B_{\rm FT}$ $(z = 0) = 1500$ G is chosen, where $z = 0$ corresponds to continuum optical depth $\tau_c = 1$ in the quiet sun. χ'_c values of 0°, 180° and 90° have been considered, i.e. canopies looking away from the limb, towards the limb, and parallel to the limb as seen by the observer (recall that by considering horizontal canopies we have chosen $\gamma'_c = 90°$). 0 and 2 km/s have been employed for $\xi_{\rm mac}$, and 0.1, 0.3 and 0.5 for $\alpha_{\rm FT}$. 0.1 is typical of $\alpha_{\rm FT}$ values obtained with low spatial-resolution data, while 0.5 can only be achieved with rather high spatial resolution data. A microturbulence of 0.8 km/s is applied in the non-magnetic portions of the atmospheres and in the canopy, while 1.0 km/s is used within the flux tubes.

3. Results

3.1. Amplitude ratios

We first discuss a selection of the results obtained with the simpler technique, i.e. from the ratio $V/\sqrt{Q^2+U^2}$.

Figure 1 shows $\Delta\gamma_{\rm FT}$ as a function of θ for $Z_c = 500$, 400 and 300 km. Plotted are results for Fe I 5250.2Å, $\alpha_{\rm FT} = 0.1$ and $\xi_{\rm mac} = 0$. We take $0 < \gamma_c < 90°$ and $\chi_c = 0$, i.e. we consider positive polarity vertical flux tubes and the canopy on the diskward side of a positive polarity sunspot. Note that for $\chi_c = 0°$ we have $\Delta\gamma_{\rm FT} = \Delta\gamma'_{\rm FT}$, i.e. the errors plotted in Fig. 1 and subsequent figures have exactly the same magnitude as the errors in the

© Kluwer Academic Publishers • Provided by the NASA Astrophysics Data System

1996SoPh..164..253S

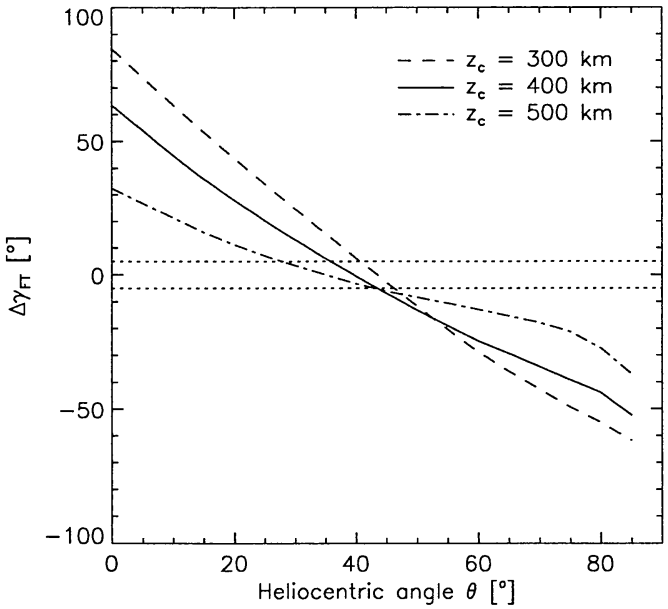

Fig. 1. Error in flux-tube inclination $\Delta\gamma_{\rm FT}$ vs. heliocentric angle θ at which the flux tube is observed. See text for a description of $\Delta\gamma_{\rm FT}$. Each curve represents $\Delta\gamma_{\rm FT}$ for a different value of the sunspot canopy base-height, $Z_{\rm c}$. Other parameters: Flux-tube magnetic filling factor $\alpha_{\rm FT} = 0.1$, spectral line Fe I 5250.2Å, flux-tube and canopy magnetic inclinations relative to line-of-sight $\gamma_{\rm FT} < 90°$, $\gamma_{\rm c} < 90°$, while the azimuths for the flux-tube and canopy fields are $\chi_{\rm FT} = 180°$ and $\chi_{\rm c} = 0$. The horizontal dotted lines bound the interval $-5° \leq \Delta\gamma_{\rm FT} \leq 5°$. The plotted results were obtained by comparing ratios of σ-amplitudes.

inclination angle relative to the surface normal. As expected $\Delta\gamma_{\rm FT}$ decreases with increasing $Z_{\rm c}$, i.e. the higher the canopy base the smaller its influence on the Stokes profiles. The qualitative dependence of $\Delta\gamma_{\rm FT}$ on θ can be understood relatively easily. For $\theta < 45°$ we have $\gamma_{\rm c} > 45° > \gamma_{\rm FT}$. Thus the combined flux-tube and canopy Stokes profiles mimic a flux tube with a larger inclination to the line-of-sight, if interpreted in terms of a flux-tube component only ($\gamma_{\rm tot} > \gamma_{\rm FT}$, i.e $\Delta\gamma_{\rm FT} > 0$). For $\theta > 45°$, on the other hand, $\gamma_{\rm c} < 45° < \gamma_{\rm FT}$, so that the combined profiles mimic flux tubes inclined towards the observer ($\gamma_{\rm tot} < \gamma_{\rm FT}$). If $B_{\rm c} = B_{\rm FT}$ then $\Delta\gamma_{\rm FT}$ must disappear at $\theta = 45°$. Since $B_{\rm c} \neq B_{\rm FT}$ and the ratio $V/\sqrt{Q^2+U^2}$ depends on the field strength (Stenflo, 1985), $\Delta\gamma_{\rm FT} = 0$ near, but not exactly at $\theta = 45°$.

The most striking feature of Fig. 1 is the magnitude of the effect. The two horizontal dotted lines lie at $|\Delta\gamma_{\rm FT}| = 5°$. We consider $\Delta\gamma_{\rm FT}$ values lying outside the area enclosed by these two lines to be significant in the sense that they are larger than the usual errors in measured flux-tube inclinations. In Fig. 1 this is the case over most of the θ range.

Figure 2 compares the results for three different values of $\alpha_{\rm FT}$: 0.1, 0.3 and 0.5 ($Z_{\rm c} = 400$ km, and the rest of the model parameters are the same as for Fig. 1). As expected $|\Delta\gamma_{\rm FT}|$ decreases strongly with increasing $\alpha_{\rm FT}$, so

© Kluwer Academic Publishers • Provided by the NASA Astrophysics Data System

1996SoPh..164..253S

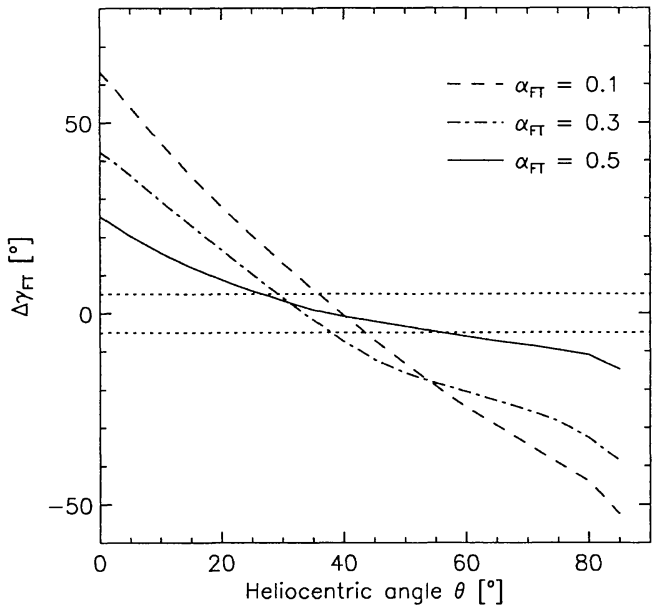

Fig. 2. Same as Fig. 1, except that each curve now represents $\Delta\gamma_{\rm FT}$ for a different $\alpha_{\rm FT}$. The height of the canopy base $Z_{\rm c} = 400$ km.

that for $\alpha_{\rm FT} = 0.5$ $|\Delta\gamma_{\rm FT}|$ remains below 5° over a θ interval of 30°. Figure 2 thus illustrates the value of high spatial resolution observations.

A non-zero $\xi_{\rm mac}$ reduces $\Delta\gamma_{\rm FT}$, since the lobes of the narrower and generally weaker canopy V and Q profiles are cancelled more readily by turbulent broadening than the flux-tube profiles. However, reasonable values of $\xi_{\rm mac}$ reduce $|\Delta\gamma_{\rm FT}|$ by only 10–20% and do not significantly modify conclusions based on calculations with $\xi_{\rm mac} = 0$.

In Fig. 3 we plot $\Delta\gamma_{\rm FT}$, determined individually from each of the three lines λ5250.2Å ($g = 3$), λ5247.1Å ($g_{\rm eff} = 2$) and λ5250.6Å ($g_{\rm eff} = 1.5$) ($Z_{\rm c} = 400$ km, $\alpha_{\rm FT} = 0.5$, $\chi_{\rm c} = 0°$ and $\gamma_{\rm c} < 90°$). $|\Delta\gamma_{\rm FT}|$ increases in the order of increasing $g_{\rm eff}$ since the strength of the canopy Q and V profiles increases relative to the flux-tube profiles for increasing $g_{\rm eff}$ (the flux-tube Q and V profiles are increasingly Zeeman saturated for increasing $g_{\rm eff}$). This implies that it is of advantage to use lines with lower $g_{\rm eff}$ to measure flux-tube inclinations.

This result may not be generalized, however, since by far the most reliable results were obtained with the most Zeeman-sensitive line in our sample, Fe I 15648Å. For the plotted case $|\Delta\gamma_{\rm FT}| < 1°$ over almost the whole θ range. This result is to a large part due to the infrared line's low height of formation (it obtains its main contribution at $\log\tau_{5000} \gtrsim -1$ in the quiet sun), which makes it rather insensitive to canopy fields with $Z_{\rm c} \gtrsim 300$ km. In addition, due to its large Zeeman sensitivity the canopy and flux-tube contributions

© Kluwer Academic Publishers • Provided by the NASA Astrophysics Data System

1996SoPh..164..253S

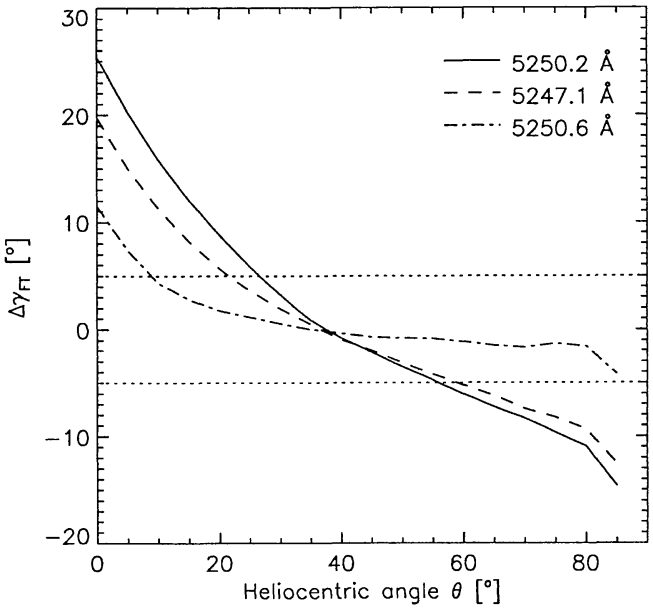

Fig. 3. Same as Fig. 1, except that each curve now represents the $\Delta\gamma_{\rm FT}$ derived from a different spectral line. We have chosen $Z_{\rm c} = 400$ km and $\alpha_{\rm FT} = 0.5$ (instead of $\alpha_{\rm FT} = 0.1$ as in Figs. 1 and 2).

to its V and Q profiles are clearly separated as a result of the different field strengths in these components (Solanki *et al.*, 1992b, 1994).

3.2. Inversions

Due to the substantially larger computing demands of the inversion technique we have applied it to a smaller model grid. We discuss only the case $Z_{\rm c} = 400$ km with $\alpha_{\rm FT} = 0.5$ and $\alpha_{\rm FT} = 0.1$.

In the upper panel of Fig. 4 we plot $\Delta\gamma_{\rm FT}$ resulting from the inversion of the combined flux-tube and canopy Stokes profiles for $\alpha_{\rm FT} = 0.5$, $Z_{\rm c} = 400$ km and three different canopy azimuths: $\chi_{\rm c}' = 0°$ (i.e. $0° < \gamma_{\rm c} \leq 90°$ and $\chi_{\rm c} = 0°$), $\chi_{\rm c}' = 90°$ (i.e. $\gamma_{\rm c} = 90°$ and $\chi_{\rm c} = 90°$) and $\chi_{\rm c}' = 180°$ (i.e. $180° > \gamma_{\rm c} \geq 90°$ and $\chi_{\rm c} = 180°$). The first of these cases corresponds, e.g., to observations on the diskward side of a sunspot with the same polarity as the flux tubes. The second case corresponds to canopy field lines lying parallel to the solar limb, as seen, e.g. when observing plage at the same θ as a nearby sunspot. The third case corresponds, e.g., to observations on the limbward side of a sunspot with the same polarity as the flux tubes. The difference to the first case ($\gamma_{\rm c} < 90°$) is that now the V profiles due to the canopy and flux-tube components have opposite signs. Each curve in Fig. 4 is based on the combined inversion of all three lines. We allowed $\alpha_{\rm FT}$, B, γ, χ and $\xi_{\rm mac}$ to be determined by the code.

© Kluwer Academic Publishers • Provided by the NASA Astrophysics Data System

1996SoPh..164..253S

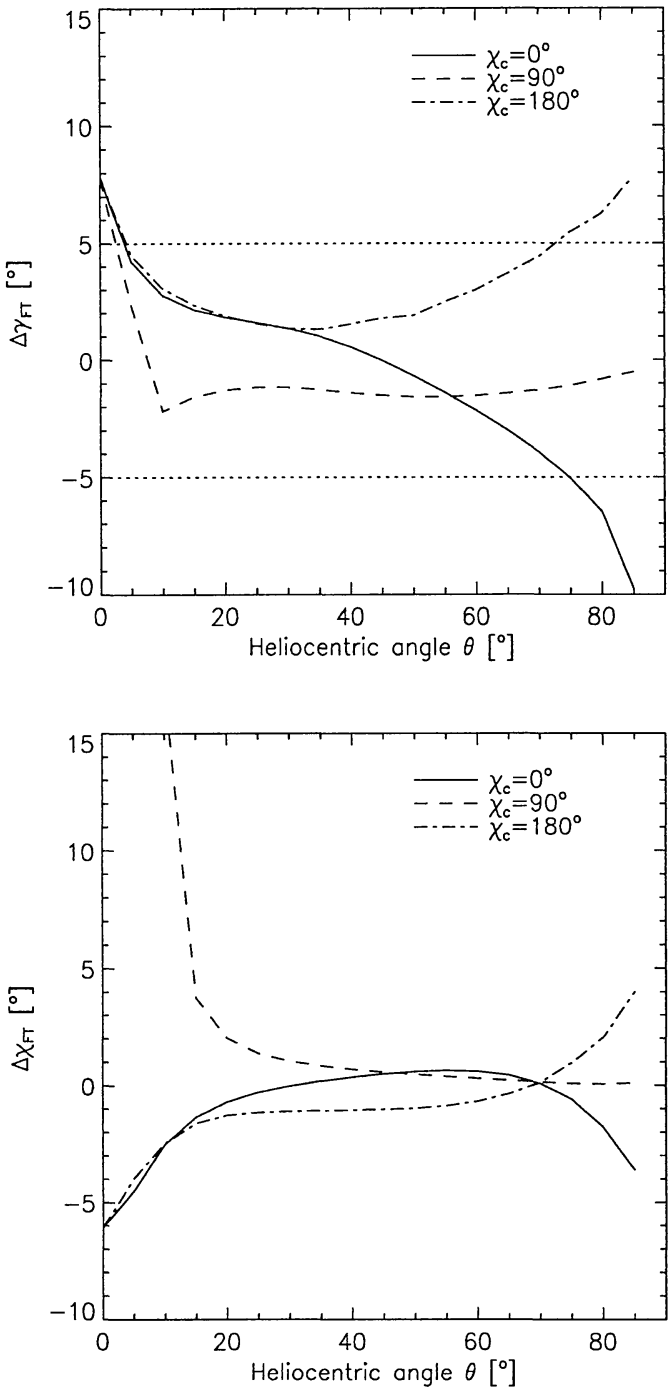

Fig. 4. Upper panel: $\Delta\gamma_{\rm FT}$ determined from multi-line inversions for three different directions of the sunspot canopy vs. θ. Solid curve: $\gamma_{\rm c} \leq 90°$, $\chi_{\rm c} = 0°$ (canopy field oriented away from the limb), dot-dashed curve: $\gamma_{\rm c} \geq 90°$, $\chi_{\rm c} = 180°$ (canopy field oriented towards the limb), and dashed curve: $\gamma_{\rm c} = 90°$, $\chi_{\rm c} = 90°$ (canopy field parallel to the limb). $\gamma_{\rm FT} < 90°$, $\chi_{\rm FT} = 180°$ in all cases. Other model parameters are $Z_{\rm c} = 400$ km and $\alpha_{\rm FT} = 0.5$. Lower panel: Error in the azimuth $\Delta\chi_{\rm FT}$ vs. θ for the same fits as in the upper panel.

© Kluwer Academic Publishers • Provided by the NASA Astrophysics Data System

1996SoPh..164..253S

A comparison between the solid curves in Figs. 2 and 4 (upper panel) indicates that the inversion technique gives on average a factor of 2–3 smaller $|\Delta\gamma_{\rm FT}|$. One reason is that the inversion code considers not only a single wavelength point but the whole line profile. It also combines fits to all three lines. Finally, the fact that the inversion determines a field strength somewhat lower than that of the flux tube (due to the canopy contribution) also plays a significant role in lowering $\Delta\gamma_{\rm FT}$. The field strength returned by the inversion code at the limb is approximately 500 G lower than the field strength of the original model flux tube. The relative strengths of the V and Q profiles of a vertical flux tube with lower B are more similar to those of the combined canopy and flux-tube profiles than the relative strengths for a strong-field flux tube.

The inversion also provides $\Delta\chi_{\rm FT}$, which is plotted in the lower panel of Fig. 4. Except near the centre of the solar disk, where $\Delta\chi_{\rm FT}$ due to the best fit tends to 90° for $\chi_{\rm c} = 90°$, $\Delta\chi_{\rm FT}$ is rather small and should not affect results significantly.

In the case plotted in Fig. 4, corresponding to very high spatial resolution measurements, sunspot canopies can for most purposes effectively be neglected, except at disk centre and at the limb. In addition, the accuracy in $\gamma_{\rm FT}$ for the parts of the canopy with field lines parallel to the limb ($\chi_{\rm c} = 90°$) is on the whole better than on the diskward and limbward sides of the sunspot.

If all parameters excluding γ and χ are fixed during the inversion, the combined inversion of all three lines results in $\Delta\gamma_{\rm FT}$ values that are intermediate between those obtained by fitting 5250.6Å alone (which gives somewhat smaller $|\Delta\gamma_{\rm FT}|$ values) and those from fitting 5250.2Å and 5247.1Å (larger $|\Delta\gamma_{\rm FT}|$ values). A simultaneous fit to all three lines is nevertheless to be preferred over fits to λ5250.6Å alone. Firstly, it gives more reliable $\chi_{\rm FT}$ values than any of the lines individually. Secondly, by fitting all three lines simultaneously we obtain in addition to $\gamma_{\rm FT}$ and $\chi_{\rm FT}$ also parameters such as field strength, macroturbulence velocity and temperature. Since each of these parameters influences the derived $\gamma_{\rm FT}$ and $\chi_{\rm FT}$, and as they are usually not known beforehand, it is important to fit multiple lines and derive all the free parameters simultaneously.

If $\alpha_{\rm FT} = 0.1$, then the $\Delta\gamma_{\rm FT}$ resulting from the inversion is quite substantial, as illustrated by Fig. 5. In this case $|\Delta\gamma_{\rm FT}| > 5°$ over a large fraction of the solar disk. The inversion nevertheless gives on average an almost two times smaller $\Delta\gamma_{\rm FT}$ than that produced by the amplitude ratio (compare with Fig. 1). Once again the inversion code underestimates the field strength of the flux-tube, which contributes to reducing $|\Delta\gamma_{\rm FT}|$ relative to the simple $V/\sqrt{Q^2+U^2}$-ratio method. The quality of the fits is not too good very close to the limb, mainly because a single magnetic component cannot properly fit the combined Stokes profiles $S_{\rm tot}$, which begin to exhibit the influence

© Kluwer Academic Publishers • Provided by the NASA Astrophysics Data System

1996SoPh..164..253S

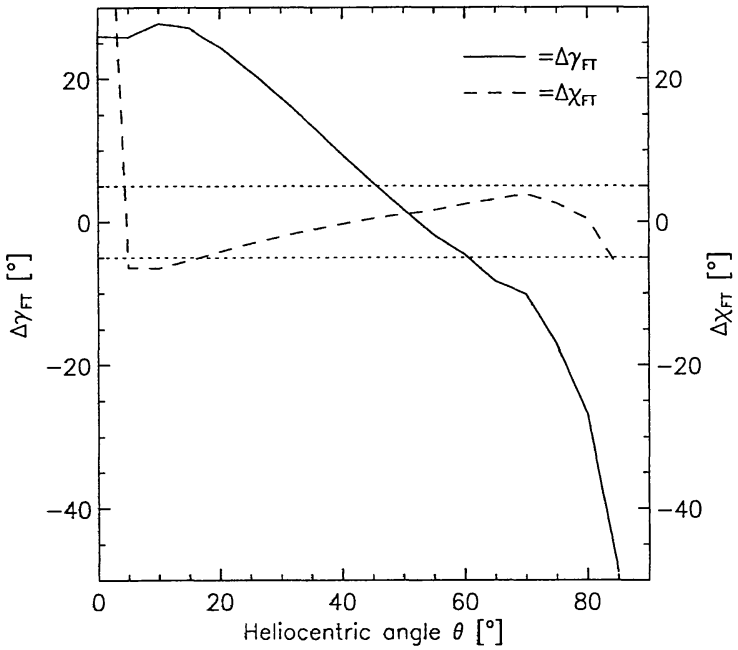

Fig. 5. $\Delta\gamma_{\rm FT}$ (solid) and $\Delta\chi_{\rm FT}$ (dashed) vs. θ for the following choice of parameters: $Z_{\rm c} = 400$ km, $\alpha_{\rm FT} = 0.1$, $\gamma_{\rm c} \leq 90°$. The diagram has been obtained by simultaneous inversion of all three visible lines.

of the second magnetic component quite clearly there. Thus, by considering only fits which reproduce the observations with high quality, it should be possible to restrict errors to less than approximately 20° in $\Delta\gamma_{\rm FT}$ due to the sunspot magnetic canopies. The error in $\gamma_{\rm FT}$ (dashed curve in Fig. 5) is once again relatively small.

4. Discussion and Conclusion

We have tested how the presence of a sunspot magnetic canopy affects measurements of the direction of the magnetic vector. The conclusions from the present work are:

1. For a line like 5250.2Å the presence of a low-lying sunspot canopy can significantly affect the flux-tube inclination derived from the observed Stokes parameters, in particular if the spatial resolution is not very high.
2. We find that an inversion approach regains the direction of the flux-tube magnetic vector more reliably than the modelling of simple line ratios.
3. The height of formation of a spectral line is important for its sensitivity to the canopy field. The lower the height of formation of a spectral line, the better it provides estimates of the flux-tube magnetic vector. In particular the Fe I 15648Å line turns out to give flux-tube magnetic

© Kluwer Academic Publishers • Provided by the NASA Astrophysics Data System

1996SoPh..164..253S

inclinations that are relatively unaffected by the canopy. For lines in the visible the error in the flux-tube inclination due to the canopy increases with increasing Zeeman sensitivity. If, however, the Zeeman sensitivity is large enough to separate the flux-tube and canopy contributions to the observed line profile, then the error in the derived inclination introduced by a sunspot canopy is also reduced.

4. Since the Stokes profiles produced by the canopy component are narrower than the flux-tube Stokes profiles (e.g. Rüedi *et al.*, 1995), we propose that it is better to observe or analyse the outer parts of the Stokes profiles in order to derive the true inclination of flux tubes, particularly when observing with an imaging instrument that has a fixed spectral passband. This choice of wavelength also possesses other advantages (cf. Jefferies & Mickey, 1991).
5. The current investigation demonstrates yet again that no diagnostic or inversion is free from model dependence and that it pays to carefully select the spectral line(s) and to consider the various possible magnetic field configurations. In other words, even the best inversion technique is no better than the underlying model and spectral diagnostics.
6. The smallest errors are achieved in the interval $\mu = \cos\theta \approx 0.5$–$0.8$. It may be worthwhile to give priority to magnetic inclination measurements in plages within roughly this range of μ values.
7. It is possible to extend the Stokes fitting technique to encompass two magnetic components (Bernasconi & Solanki, 1995) and thus model the effect of the canopy directly during the inversion. This may be a promising approach for the future.

The relevance of the current investigation to the real sun depends on the fraction of plage area covered by low-lying sunspot canopies. Giovanelli & Jones (1982) found for two active regions that approximately half of the surface area free from magnetic fields in the low photosphere is covered by nearly horizontal canopies with a base height below 500 km. Although it is not obvious how closely their canopy base height corresponds to ours, it is nevertheless clear that the influence of sunspot canopies cannot be neglected in active regions.

Sunspot magnetic canopies may thus affect magnetic inclination measurements of the type presented by Solanki *et al.* (1987), Lites & Skumanich (1990) and Bernasconi *et al.* (1995), all of which have low spatial resolution.* We suggest that in order to deliver more reliable values of $\gamma_{\rm FT}$ and $\chi_{\rm FT}$ future Stokes vector measurements in plages should either make use of high spatial resolution, employ lines formed low in the atmosphere (e.g. Fe I 15648Å),

* The results of Lites & Skumanich (1990), being based on Fe I 6302.5Å, which has a somewhat lower height of formation than the Fe I lines around 5250Å favoured by the other investigators, probably are somewhat less affected by sunspot canopies.

© Kluwer Academic Publishers • Provided by the NASA Astrophysics Data System

1996SoPh..164..253S

or include the influence of a possible sunspot canopy directly in the model on which the inversion is based.

References

Bernasconi P.N., Solanki S.K.: 1995, *Solar Phys.* in press

Bernasconi P.N., Keller C.U., Povel H.P., Stenflo J.O.: 1995, *Astron. Astrophys.* in press

Bruls J.H.M.J., Solanki S.K., Carlsson M., Rutten R.J.: 1995, *Astron. Astrophys.* **293**, 225

Cattaneo F., Hurlburt N.E., Toomre J.: 1990, *Astrophys. J.* **349**, L63

Defouw R.J., 1976, *Astrophys. J.* **209**, 266

Finsterle, W.: 1995, *Bestimmung der Magnetischen Struktur von Sonnenflecken mit Infrarot und Optischen Spektren (in German),* Diplomarbeit, Institute of Astronomy, ETH, Zürich

Giovanelli R.G.: 1980, *Solar Phys.* **68**, 49

Giovanelli R.G., Jones H.P.: 1982, *Solar Phys.* **79**, 267

Hewagama T., Deming D., Jennings D.E., Osherovich V., Wiedemann G., Zipoy D., Mickey D.L., Garcia H., 1993, *Astrophys. J. Suppl. Ser.* **86**, 313

Howard R.F.: 1991, *Solar Phys.* **134**, 233

Jefferies J.T., Mickey D.L.: 1991, *Astrophys. J.* **372**, 694

Jones H.P., Giovanelli R.G., 1983, *Solar Phys.* **87**, 37

Lites B.W., Skumanich A.: 1990, *Astrophys. J.* **348**, 747

Maltby P., Avrett E.H., Carlsson M., Kjeldseth-Moe O., Kurucz R.L., Loeser R.: 1986, *Astrophys. J.* **306**, 284

Murphy G.A.: 1990, *The Synthesis and Inversion of Stokes Spectral Profiles*, NCAR Cooperative Thesis No. 124

Murray N.: 1992, *Astrophys. J.* **401**, 386

Nesis A., Bogdan T.J., Cattaneo F., Hanslmeier A., Knölker M., Malagoli A., 1992, *Astrophys. J.* **399**, L99

Rees D.E., Murphy G.A., Durrant C.J.: 1989, *Astrophys. J.* **339**, 1093

Rüedi I., Solanki S.K., Livingston W., Stenflo, J.O.: 1992, *Astron. Astrophys.* **263**, 323

Rüedi I., Solanki S.K., Livingston W., 1995, *Astron. Astrophys.* **293**, 252

Sánchez Almeida J., Martínez Pillet V.: 1994, *Astrophys. J.* **424**, 1014

Schüssler M.: 1986, in *Small Scale Magnetic Flux Concentrations in the Solar Photosphere*, W. Deinzer, M. Knölker, H.H. Voigt (Eds.), Vandenhoeck & Ruprecht, Göttingen, p. 103

Schüssler M.: 1990, in *Solar Photosphere: Structure, Convection and Magnetic Fields*, J.O. Stenflo (Ed.), Kluwer, Dordrecht, *IAU Symp.* **138**, 161

Solanki S.K.: 1993, *Space Science Rev.* **61**, 1

Solanki S.K., Brigljević V.: 1992, *Astron. Astrophys.* **262**, L29

Solanki S.K., Keller C., Stenflo J.O.: 1987, *Astron. Astrophys.* **188**, 183

Solanki S.K., Rüedi I., Livingston W.: 1992a, *Astron. Astrophys.* **263**, 312

Solanki S.K., Rüedi I., Livingston W.: 1992b, *Astron. Astrophys.* **263**, 339

Solanki S.K., Montavon C.A.P., Livingston W.: 1994, *Astron. Astrophys.* **283**, 221

Solanki S.K., Rüedi I., Bianda M., Steffen M.: 1995a, *Astron. Astrophys.* submitted

Solanki S.K., Steiner O., Bünte M., Murphy G.: 1995b, *Astron. Astrophys.* to be submitted

Steiner O., Grossmann-Doerth U., Knölker M., Schüssler M.: 1995, *Rev. Mod. Astron.* **8**, p. 81

Stenflo J.O.: 1985, in *Measurements of Solar Vector Magnetic Fields*, M.J. Hagyard (Ed.), NASA Conf. Publ. 2374, p. 263

Stenflo J.O., Solanki S.K., Harvey J.W., 1987, *Astron. Astrophys.* **171**, 305

Zayer I., Solanki S.K., Stenflo J.O., Keller C.U., 1990, *Astron. Astrophys.* **239**, 356

© Kluwer Academic Publishers • Provided by the NASA Astrophysics Data System